The Relationship between Nightside O^+ Outflow and Sawtooth Events

N. Nowrouzi[1], E. J. Lund[1,2], L. M. Kistler[1]

[1]University of New Hampshire, [2]College Brook Scientific

GEM, 2017

Poster # 33

Introduction and Motivation

- Sawtooth events are repeated injections of energetic particles at geosynchronous orbit
- 94% of sawtooth events occur during geomagnetic storms [Cai et al., 2011]
- O^+ in the tail has been suggested as a possible driver
- Simulations [Brambles et al., 2013] suggest that O^+ from nightside ionosphere produces a feedback that drives subsequent injections in ICME-driven events

This study tests observational support for this idea. Using data from the FAST satellite from 1997-1998, we:

1. Determine auroral boundaries [Andersson et al., 2004]
2. Calculate O^+ outflow flux
3. Determine the profile of auroral O^+ outflow by superposed epoch analysis with respect to injection time and test to see any difference between them and isolated substorm ones. [Wilson et al., 2004]

Sample Sawtooth Event

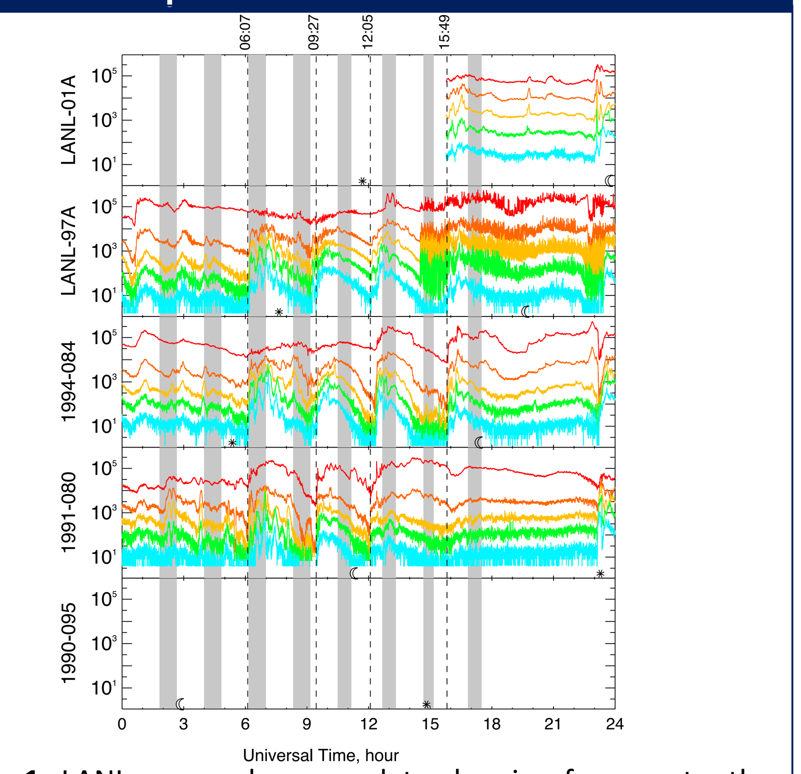

Figure 1. LANL geosynchronous data showing four sawtooth injections during the event. Injection time is marked by dashed blue lines. FAST passes are shaded by gray bars

Auroral Boundaries

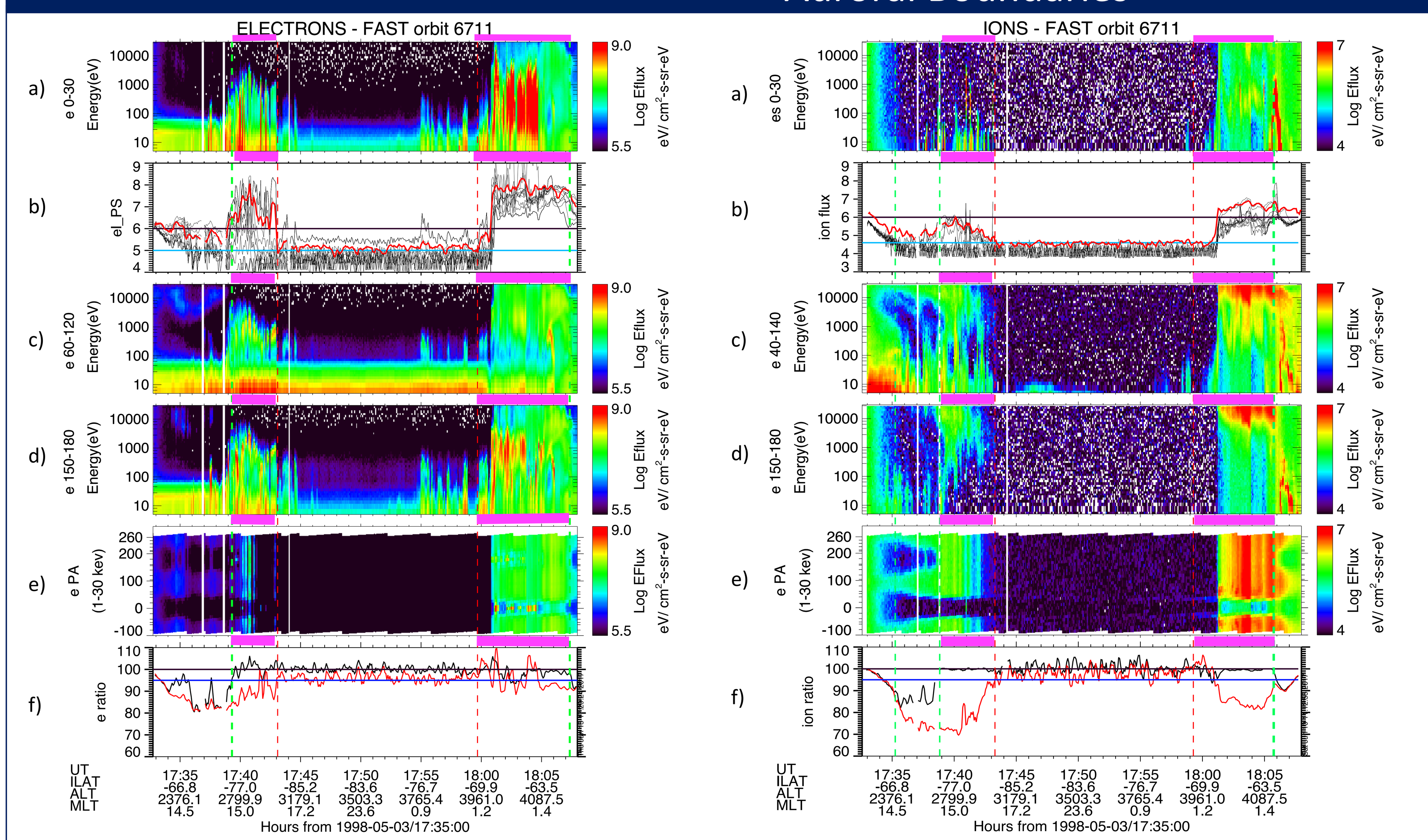

Criteria to determine the boundaries

- **Equatorward Boundaries**

Inner edge equatorward boundary: The time when the earthward to perpendicular flux ratio starts to diverge from the antiearthward to perpendicular flux ratio

Outer edge equatorward boundary: The time when the earthward flux ratio reaches a value of 95 percent or higher.

- **Poleward edge boundary**

The most equatorward location at which the mean flux level drops below $10^{4.6}$ eV/(cm² s sr eV) for the ions from the IESA and 10^5 for electrons from EESA instrument for more than 10 s.

Figure 2. Particle spectra observed from orbit 2000 by the FAST space craft. (a) Earthward energy spectrogram flux of electron, (c) Perpendicular, (d) Antiearthward, (b) line plot of energy flux versus time for representative energy and pitch angle channels (black lines) and the mean measure flux calculated from Figures 1a, 1c, 1d., (e) Particle flux as a function of pitch angle and time/space for the integrated energy range of 1-30 keV, (f) the ratio between the filed-aligned and perpendicular fluxes. The black line presents the Earthward ration and the red line presents the Antiearthward ratio. The green vertical lines represent the equatorward location of the auroral oval and the red vertical lines represent the polar cap boundary.

O+ Outflow Flux

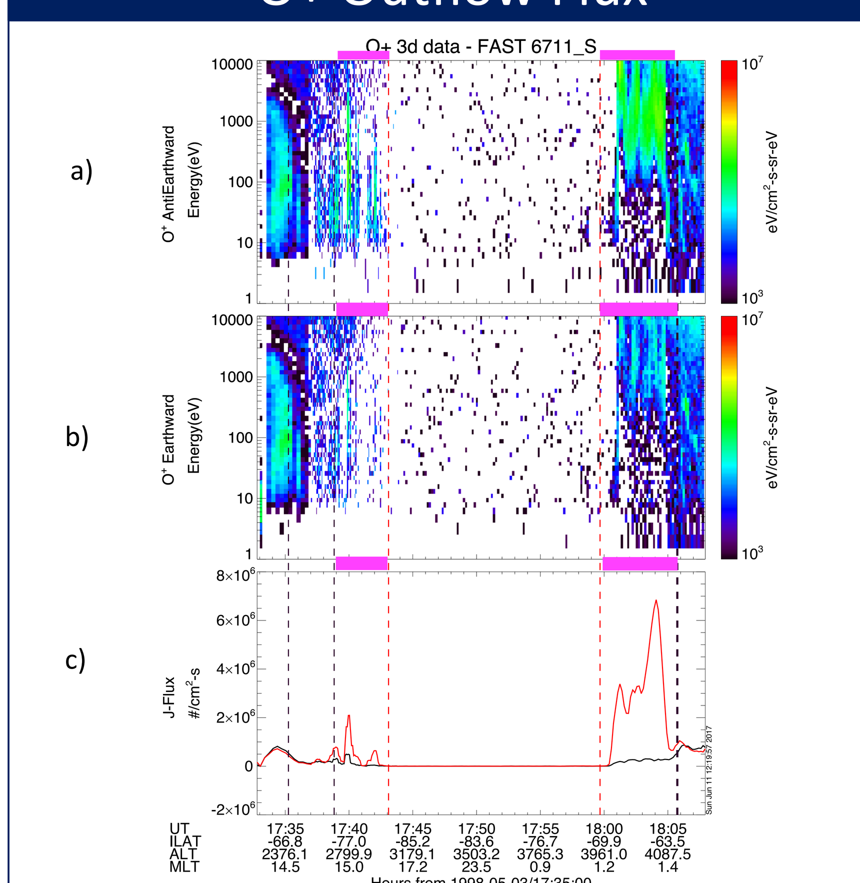

Figure 3. (a) Antiearthward spectrogarm energy flux of O^+ ion outflow, (b) earthward spectrogram energy flux of O^+ ion outflow, (c) The number flux of antiearthward and earhward O+ outflow

Polar UVI Auroral Luminosity

Figure 4. Images from 17 small substorms were averaged together to produce this sequence of 40 composite images spanning the time from 30 min before the onset and 90 min after the onset. Each composite image covers a 3 min interval. Inner and outer circle show the 70 and 50 magnetic altitude, respectively. Onset occurs between image 10 and image 11.(Wilson et al. 2004)

- Dividing substorms into two groups(group1: small substorms and group2: large substorms)
- Binning the time from 30 min before the onset and 90 min after the onset into 3 minutes interval and getting averages of images to make a composite image of auroral luminosity
- Finding the area of polar cap and nightside auroral zone as a function of time.
- Calculating the average flux by using 30 min time bins
- Calculating O^+ outflow rate by multiplying the area of zones and their average outflow fluxes.

Table 1*. Average Ion Flux($cm^{-2}\,s^{-1}$)

	Group 1		Group 2		Group 1		Group 2	
Δt, min	Flux	Number	Flux	Number	Flux	Number	Flux	Number
	Nightside Auroral Zone O^+				*Nightside Auroral Zone H^+*			
−30–0	3.2×10^6	552	4.0×10^6	557	3.1×10^6	552	7.3×10^6	557
0–30	4.5×10^6	649	5.6×10^6	761	6.8×10^6	649	1.1×10^7	761
30–60	3.8×10^6	680	4.8×10^6	1163	8.7×10^6	680	5.6×10^6	1163
60–90	1.9×10^6	347	4.5×10^6	115	3.6×10^6	347	1.1×10^7	115
	Polar Cap O^+				*Polar Cap H^+*			
−30–0	4.3×10^5	417	6.7×10^5	560	1.4×10^5	417	4.1×10^5	560
0–30	2.9×10^5	657	2.4×10^5	571	4.4×10^5	657	2.8×10^5	571
30–60	5.6×10^5	596	1.8×10^5	275	5.8×10^5	596	5.5×10^4	275
60–90	4.7×10^5	228	2.9×10^5	124	3.5×10^5	228	5.6×10^5	124

* (Wilson et al. 2004)

Outflow Rate

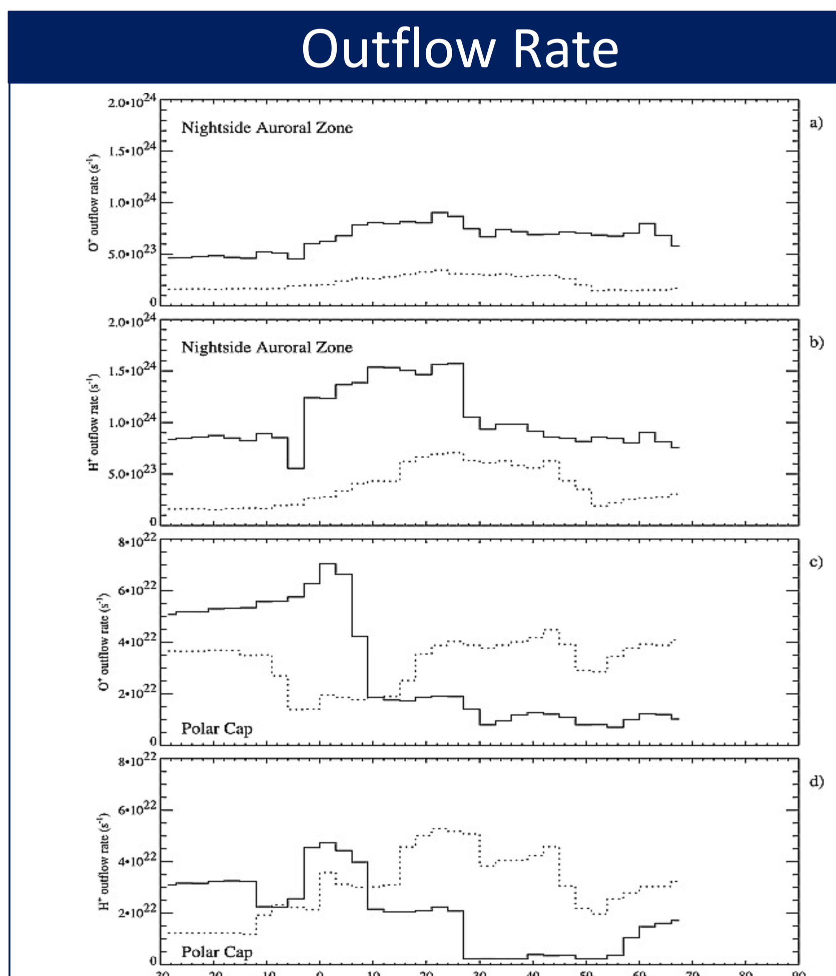

Figure 5.(a) Nightside auroral zone (a) O^+ outflow rate and (b) H^+ and Polar cap zone (c) O^+ outflow rate and (d) H^+ outflow rate as a function of time from onset. (Wilson et al. 2004)

Fast Trajectory during Sawtooth Events

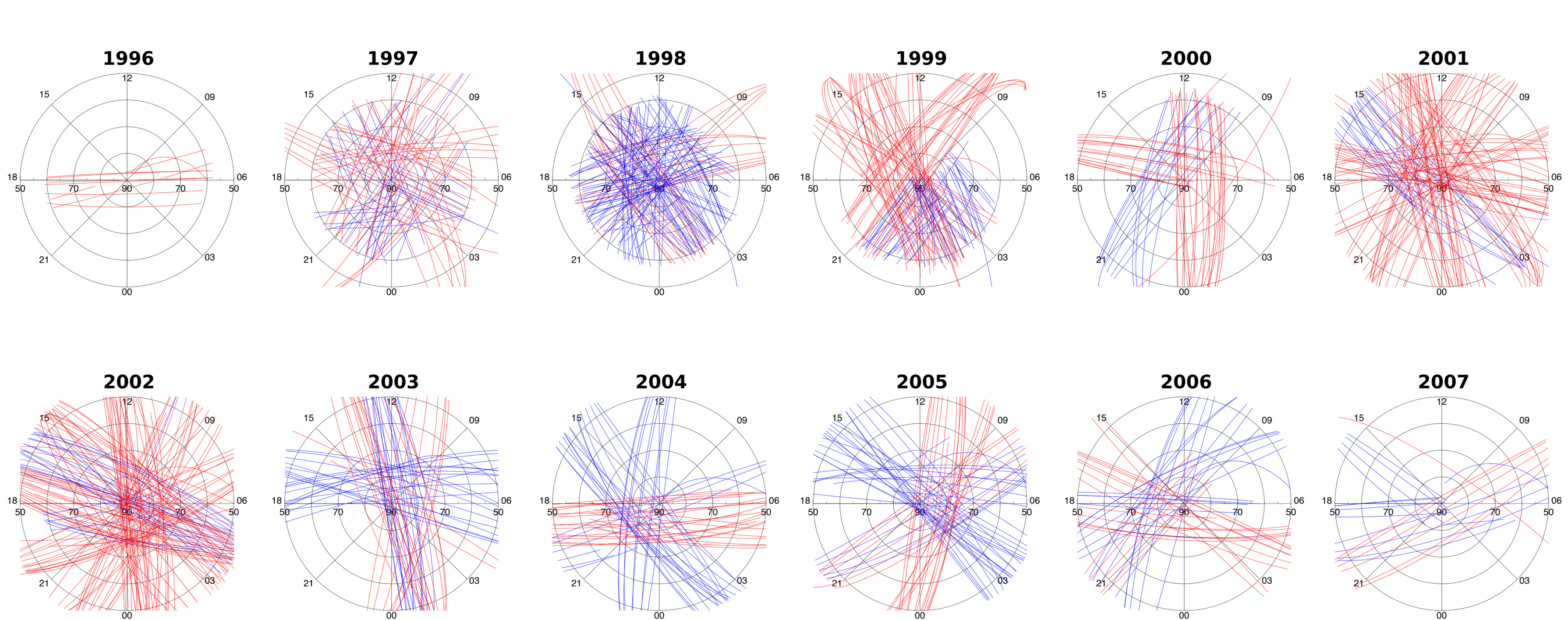

Figure 6. FAST trajectories for the sawtooth events of the year of 1997 and 1998 from the polar region. Northern hemisphere passes are in blue and southern hemispheric passes are in red.

Preliminary Result

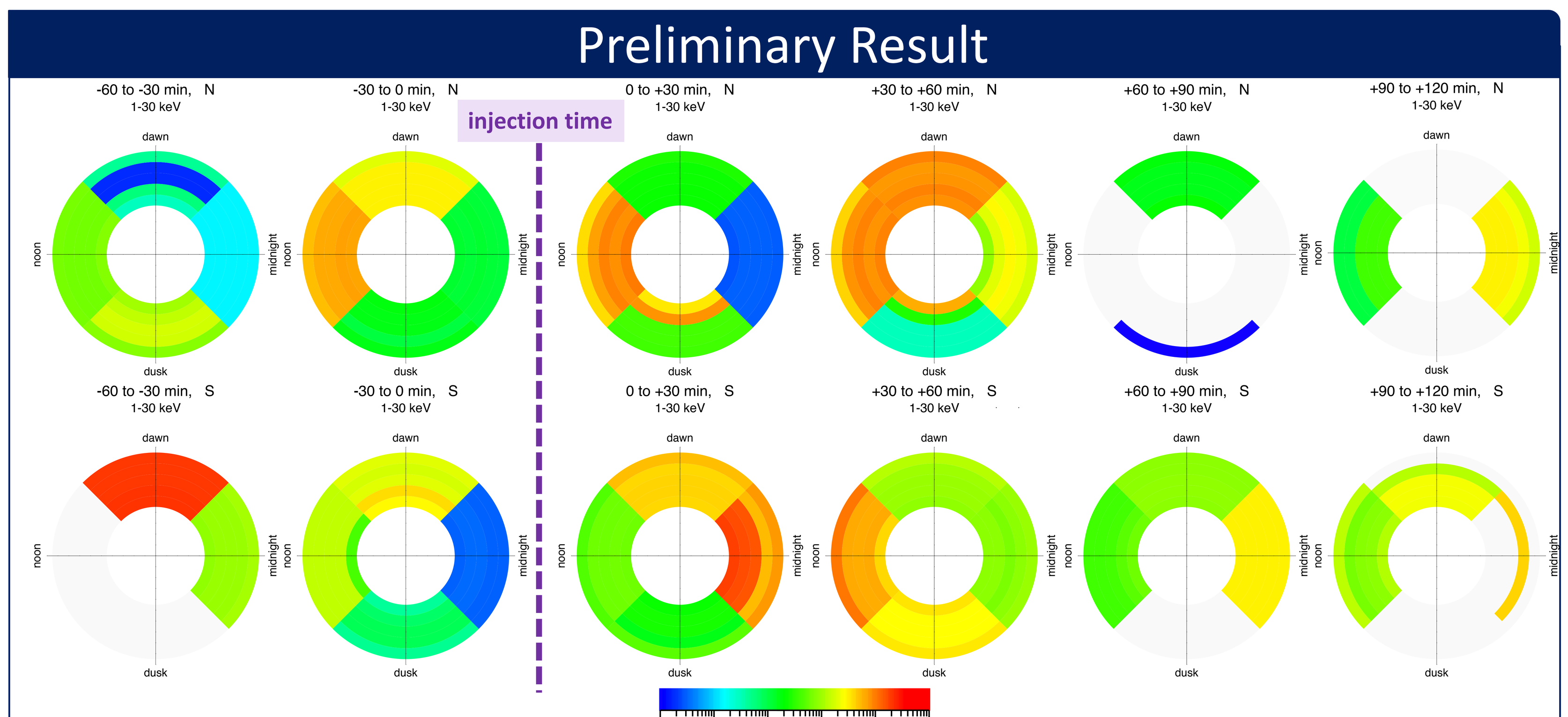

Figure7: O+ outflow flux from the sawtooth events are averaged, as a function of the Magnetic Local Time (MLT) and their place inside the auroral region, from 1997 to 1998. These plots are showing an averaged 30-minute interval from 60 min before the injection to 120 min after the injection time of each tooth, each plot showing an averaged 30-minute interval. O+ outflow flux is coming from the northern hemisphere in the first row and from the southern hemisphere in the second row.

Summary

- Using EESA and IESA FAST data, the poleward and the equatorward auroral boundaries for each FAST pass through the polar region are determined.
- Using TEAMS data, the outflow O^+ flux inside the auroral zone is calculated.
- Applying superposed epoch analysis, the changes of O+ outflow during the sawtooth events from 1997 to 1998 are tested via binning into 30-minute intervals. The averaging over the O+ outflow flux for each bin is done as a function of MLT and their location inside the auroral zone.
- After validating these results, we are going to extend this method to examine the O+ outflow from 1996 to 2007.

References

Andersson et al. [2004], JGR 109, A08201, doi:10.1029/2004JA010424
Andersson et al.[2005], JGR 32, L09104, doi:10.1029/2004GL021434
Brambles et al. [2011], Science 332, 1183, doi: 10.1126/science.1202869
Brambles et al. [2013], JGR 114, A06201, 10.1002/jgra.50522
Cai et al. [2011], JGR 116, A07208, doi: 10.1029/2010JA016310
Wilson et al.[2004],JGR 109, A02206, doi:10.1029/JA009835